



Hassouna, S., Rains, J., Kazim, J. U. R. , Ur Rehman, M. , Imran, M. and Abbasi, Q. H. (2022) Discrete Phase Shifts for Intelligent Reflecting Surfaces in OFDM Communications. In: International Workshop on Antenna Technology (iWAT2022), Dublin, Ireland, 16-18 May 2022, ISBN 9781665494502 (doi: [10.1109/iWAT54881.2022.9810915](https://doi.org/10.1109/iWAT54881.2022.9810915))

The material cannot be used for any other purpose without further permission of the publisher and is for private use only.

There may be differences between this version and the published version. You are advised to consult the publisher's version if you wish to cite from it.

<http://eprints.gla.ac.uk/266659/>

Deposited on 07 March 2022

Enlighten – Research publications by members of the University of Glasgow

<http://eprints.gla.ac.uk>

# Discrete Phase Shifts for Intelligent Reflecting Surfaces in OFDM Communications

1<sup>st</sup> Saber Hassouna

*James Watt School of Engineering  
University of Glasgow  
Glasgow,UK  
s.hassouna.1@research.gla.ac.uk*

2<sup>nd</sup> James Rains

*James Watt School of Engineering  
University of Glasgow  
Glasgow,UK  
j.rains.1@research.gla.ac.uk*

3<sup>rd</sup> Jalil ur Rehman Kazim

*James Watt School of Engineering  
University of Glasgow  
Glasgow,UK  
j.kazim.1@research.gla.ac.uk*

4<sup>th</sup> Masood Ur Rehman

*James Watt School of Engineering  
University of Glasgow  
Glasgow,UK  
Masood.UrRehman@glasgow.ac.uk*

5<sup>th</sup> Muhammad Imran

*James Watt School of Engineering  
University of Glasgow  
Glasgow,UK  
muhammad.imran@glasgow.ac.uk*

6<sup>th</sup> Qammer H. Abbasi

*James Watt School of Engineering  
University of Glasgow  
Glasgow,UK  
qammer.abbasi@glasgow.ac.uk*

**Abstract**—Reconfigurable intelligent surface (RIS) in wireless communications allows the network provider to control the scattering, reflection, and refraction characteristics of the electromagnetic signals. Different research results have shown (RIS) can effectively control the properties of the wireless waves like Amplitude and Phase without complex equalization and decoding at the receiver. Nevertheless, configuring the surface under practical frequency selective fading channel must be considered over the whole bandwidth consequently we took into consideration the wideband orthogonal frequency division multiplexing (OFDM) communication system based on practical (RIS) setup with different phase shifts per each element in the surface. We used the communication setup considered in the IEEE signal processing Cup 2021 to investigate the user data rate enhancement of such (RIS) surfaces using different discrete phase shifts with equal spacing. Simulation results shown that the data rate improved when using high resolution of discrete phase shifts per each RIS element.

**Index Terms**—Reconfigurable intelligent surface (RIS), Intelligent reflecting surface (IRS), orthogonal frequency division multiplexing (OFDM), Reflection Coefficient and Discrete phase shifts

## I. INTRODUCTION

Recently, a new technology was emerged into the wireless communication research: reconfigurable intelligent surfaces (RISs). The RISs are intelligent surfaces which are manufactured from electromagnetic materials (EM). The materials are controlled by microelectronic circuits that have the features of wireless communications and hence managing the wireless propagations scenarios in a way that was not discovered in the prior research [1]–[3]. The RISs consist of an enormous number of small low cost and passive components (elements) that are fit for changing the wireless signals impinging upon them in manners that normal materials and surfaces are not able to do. By and large, it is significant to mention that previous research has predominantly considered frequency flat fading channels for narrowband communications, where reflection coefficients of the IRS are designed to adjust the

phase of base station BS-IRS-User reflected path with the BS user direct path for construction interference. When frequency-selective fading channels are considered, however, the IRS reflection coefficients must cater to all signal paths at various delays, making optimization problems more difficult to solve, whereas different subcarriers in orthogonal frequency division multiplexing (OFDM) systems prefer different configurations over a single configuration, making RIS less effective [4]. In [5], heuristic techniques of different complexity are given for combined channel estimate and IRS configuration for OFDM systems. Prior research has assumed that IRS elements can be perfectly tuned to have a constant amplitude and continuous phase configuration. A practical IRS may not meet any of these ideal parameters [6], necessitating the development of novel solutions.

In this study, we use data set from the IEEE Signal Processing Cup 2021 [7] to investigate the performance gains at different phase shifts around 0 and 180 or -180 degree using an OFDM system but for different phase shifts than the proposed in [6]. We investigated three bits RIS system to check the impact on the user data rate for the line of sight (LOS) and Non-line of sight (NLOS) user equipment's and compare it with the first bit and the random phase RIS. The greater the range of discrete phases you consider, the more data rate enhancement, but at the cost of hardware complexity. The following is a summary of the rest of the paper. The system model and OFDM transmission are introduced in Section II. The practical phase shift model is the focus of Section III, which concludes with the simulation results. Finally, in part IV, there is a conclusion.

## II. SYSTEM MODEL

We discuss communication from a single antenna source (AP) to many users' equipment's (UEs) using an IRS with Nreconfigurable controllable elements. We assume the transmission is carried out using OFDM with a unit energy sinc-

function as the pulse shape filter as in the model derived in [3].  $x(t)$  is the transmitted discrete time signal in the complex baseband domain then the corresponding received discrete time signal sequence  $z[k]$  is given by:

$$z[k] = \sum_{l=0}^{M-1} h_{\theta}[l]x[k-l] + w[k] \quad (1)$$

Where  $\{h_{\theta}[l] : l = 0, \dots, M-1\}$  is the finite impulse response (FIR) filter that describe the wideband channel in the time domain with the IRS configuration  $\theta$  and  $\{w[k]\}$  is the receiver noise.  $h_{\theta}[l]$  is given by:

$$h_{\theta}[l] = h_d[l] + v_l^T w_{\theta} \quad (2)$$

Where  $h_d[l]$  is the uncontrollable channel,  $v_l \in \mathbb{C}^N$  is the cascaded channels via each of the  $N$  elements and  $w_{\theta} \in \mathbb{C}^N$  contains the actual reflection coefficients of the IRS that determine the amplitude losses and phase shifts. We use OFDM transmission with cyclic prefix (CP) length  $M-1$  and creates  $K > M$  subcarriers so, a block of  $K+M-1$  time domain signals are transmitted to create one OFDM block with  $K$  parallel subcarriers using the discrete Fourier transform (DFT):

$$\bar{z} = \bar{h}_{\theta} \odot \bar{x} + \bar{w} \quad (3)$$

Where  $\odot$  denotes the Hadamard product and all the vectors are of length  $K$  and  $\bar{h}_{\theta}$  is realized as follows:

$$\bar{h}_{\theta} = F \begin{bmatrix} h_d[0] + v_0^T w_{\theta} \\ \vdots \\ h_d[M-1] + v_{M-1}^T w_{\theta} \end{bmatrix} = F (h_d + V^T w_{\theta}) \quad (4)$$

Where  $h_d = [h_d[0], \dots, h_d[M-1]]^T$  represents all the uncontrollable channel components,  $V = [v_0, \dots, v_{M-1}] \in \mathbb{C}^{N \times M}$  gathers all the components containing the controllable propagation channels and  $F$  is a  $K \times M$  DFT Matrix with the  $(v, k)$ th element being  $e^{-\frac{2\pi kv}{K}}$ . As a result, the sum rate over the subcarriers is given as [3] for a given configuration, equal power allocation, and perfect channel estimate at the receiver:

$$R = \frac{B}{K+M-1} \sum_{v=0}^{K-1} \log_2 \left( 1 + \frac{P |\bar{h}_{\theta}[v]|^2}{BN_o} \right) \frac{\text{bit}}{s} \quad (5)$$

Where  $B$  is the channel bandwidth,  $P$  is the transmit power and  $N_o$  is the noise power spectral density (i.e.  $\bar{w}[k] \sim N_c(0, N_o)$ ). The rate can be maximized with respect to  $\theta$ . We will investigate the rate performance in the same setup in [6] but considering higher phase resolutions per element in the surface. We consider the deployment scenario which is the same of the signal Cup [7]. The IRS is deployed to feature line-of-sight (LOS) propagation from the access point (AP) and also to most of the User Equipment, but we will also consider the case of NLOS propagation, which could happen when the LOS path is blocked by some object close to the UE. The channel parameters values are generated by adopting the 3GPP model [8] where the number of subcarriers  $K = 500$  and the channel Taps  $M = 20$  Taps and the number of users

(UE's) are 50 users, 14 of them are NLOS users while the others are LOS users.

### III. PRACTICAL PHASE SHIFT MODEL

#### A. Equivalent Circuit Model

The analogous model for the  $n$ th reflecting element is a parallel resonant circuit with an impedance of [9]:

$$Z_n(C_n, R_n) = \frac{j\omega L_1 \left( j\omega L_2 + \frac{1}{j\omega C_n} + R_n \right)}{j\omega L_1 + \left( j\omega L_2 + \frac{1}{j\omega C_n} + R_n \right)} \quad (6)$$

The bottom layer inductance, top layer inductance, effective capacitance, effective resistance, and angular frequency of the incident signal are represented as  $L_1, L_2, C_n, R_n$  and  $\omega$  respectively. The fraction of the reflected electromagnetic wave due to the impedance discontinuity between the free space impedance  $Z_o$  and the element impedance  $Z_n(C_n, R_n)$  is described by the reflection coefficient:

$$v_n = \frac{Z_n(C_n, R_n) - Z_o}{Z_n(C_n, R_n) + Z_o} \quad (7)$$

Because  $v_n$  is a function of  $C_n, R_n$  and  $\omega$ , the reflected (EM) waves may be controlled and programmed by altering the values of  $C_n, R_n$  and  $\omega$ . Values of  $C_n$ , which range from 0.15pF to 1.5pF,  $R_n = 1\text{ohm}$ ,  $Z_o = 377\Omega$  is the free space impedance, and  $f = 4\text{GHz}$ , respectively. If a sinusoidal signal with frequency  $f$  impinging the IRS element, it will be scattered with an amplitude change of  $|v_n|$  and phase shift of  $\arg(v_n)$ . The IRS is controlled by different numbers of PIN diodes dedicated per each element for instance we need one PIN diode for each element in case of one-bit RIS while two and three PINs for two and three bits respectively. Each PIN Diode can take two different values of ON and OFF capacitances. In this study, we investigate the data rate per user for various pairings of capacitance values that correspond to different reflecting phase shifts per IRS element. Fig (1) shows the amplitude and phase of the reflection coefficient at the carrier frequency  $f = 4\text{GHz}$ . Each capacitance value provides different reflecting phase shift for example the values of the capacitances 0.5011pF and 0.3732pF are corresponding to the phases -90 and 90 degrees respectively which will result to 180-degree phase shift spacing per element as per Table I.

The reflection Coefficients with IRS involvement become:

$$w_{\theta} = \begin{bmatrix} v(C_1, f_c) \\ \vdots \\ v(C_N, f_c) \end{bmatrix} \quad (8)$$

#### B. Channel Estimation and IRS Configuration

The capacity is obtained by maximizing the sum data rate in (5) with respect to both the power allocation and RIS configuration. The former is a classical problem with a solution called water filling (WF) power allocation:

$$P_v = \max \left( \mu - \frac{BN_o}{|f_v^H h_d + f_v^H V^T w_{\theta}|^2}, 0 \right) \quad (9)$$

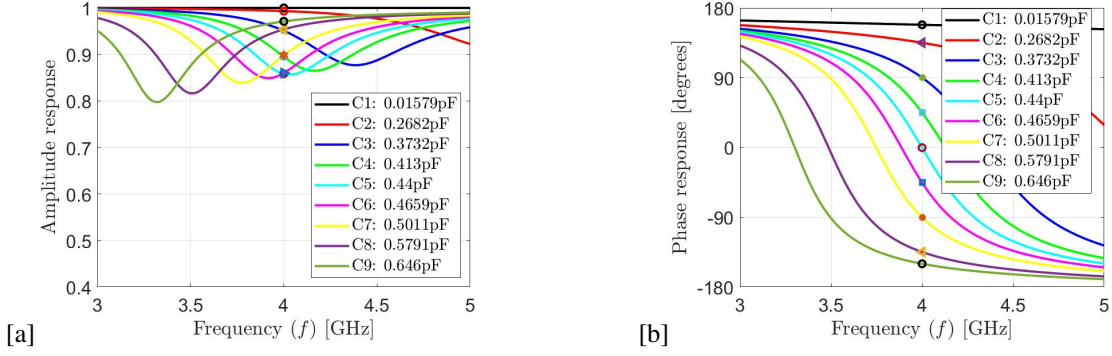


Fig. 1. Amplitude and Phase Response of the reflection coefficient  $v_n$ .

TABLE I  
DISCRETE PHASE SHIFTS FOR IRS

RIS Type	Phase in Degree	Capacitance in Farad	Configuration
<b>1 bit</b>	-90	0.501pF	<b>1</b>
	90	0.37pF	<b>0</b>
<b>2 bits</b>	0	0.44pF	<b>00</b>
	90	0.37pF	<b>10</b>
	180	0.1pF	<b>10</b>
	270	0.501pF	<b>11</b>
<b>3 bits</b>	0	0.44pF	<b>000</b>
	45	0.413pF	<b>001</b>
	90	0.37pF	<b>010</b>
	135	0.268pF	<b>011</b>
	180	0.1pF	<b>100</b>
	225	0.58pF	<b>101</b>
	270	0.501pF	<b>110</b>
	315	0.466pF	<b>111</b>

Where the parameter  $\mu \geq 0$  is selected to make  $\frac{1}{K} \sum_{v=0}^{K-1} P_v = P$  and  $f_v^H$  is the  $v$ th row of the DFT matrix  $F$ . The maximization of (5) with respect to the RIS configuration  $\theta$  entails selecting the most optimal vector  $w_\theta$  which is affecting all the subcarriers because the transmissions are simultaneous. Consequently, channel estimation is required and since the IRS is passive, the estimation must be carried out at the receiver. Consequently, the least square (LS) estimate can be calculated as follows [3]:

$$\left[ \hat{h}_d, \hat{V}_{\text{row}}^T \right] = \sqrt{\frac{B}{P}} F^\dagger Z \left[ \begin{array}{c} 1, \dots, 1 \\ A^T \hat{\Omega} \end{array} \right]^\dagger \quad (10)$$

Where  $A = (1_{N_V} \otimes I_{N_H}) \in \mathbb{C}^{N_X N_H}$  is the reduced matrix,  $N_N$  and  $N_H$  is the number of IRS vertical and horizontal elements respectively,  $Z = [\bar{z}_1, \dots, \bar{z}_c] \in \mathbb{C}^{N_X C}$  contains all the received signals and  $\dagger$  denotes Moore-Penrose inverse. The maximization of  $\hat{h}_d$  and  $\hat{V}_{\text{row}}^T$  with respect to the RIS configuration needs selecting the most preferred vector  $\hat{\Omega} = [w_{\theta_1}, \dots, w, w_{\theta_c}]$ . The literature contains heuristic approaches based on successive convex approximation, semidefinite relaxation, and strongest tap maximization (STM) in the time domain [3], [4]. however, we will utilize the identical approach in [6] to make sure it works for both LOS and NLOS channels with differing reflecting phase shifts and hence different RIS

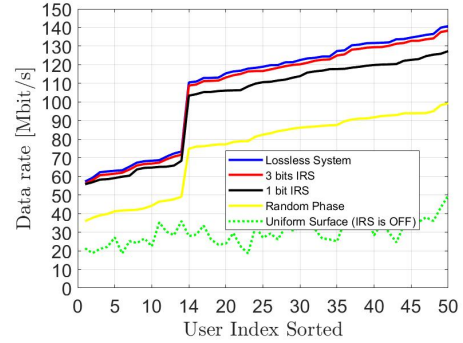


Fig. 2. The data rates when considering different types of RIS and compared with the uniform surface (The RIS is OFF)

types. The power method algorithm is utilized to find the maximum dominant eigen vector of the matrix to be the optimal solution. The received signal power can be represented in a quadratic form where the number of iterations has to be completed until convergence. The received signal power [6] is proportional to:

$$\| \bar{h}_\theta \|^2 = \left[ \frac{1}{\frac{A^T w_\theta}{N_V}} \right]^H [h_d, N_V V_{\text{row}}^T]^H [h_d, N_V V_{\text{row}}^T] \left[ \frac{1}{\frac{A^T w_\theta}{N_V}} \right] \quad (11)$$

Where  $N_N$  and  $N_H$  is the number of IRS vertical and horizontal elements respectively,  $[...]^H$  is hermitian matrix,  $A = (1_{N_V} \otimes I_{N_H}) \in \mathbb{C}^{N_X N_H}$ ,  $\otimes$  denotes the Kronecker product,  $1_{N_H} = [1, \dots, 1]^T \in \mathbb{C}^{N_H}$  and  $V_{\text{row}} \in \mathbb{C}^{N_H X M}$  is the reduced dimension matrix that captures the channel coefficients for any row of the IRS. Let us consider  $C = \left[ \frac{1}{\frac{A^T w_\theta}{N_V}} \right]$  and  $b = [h_d, N_V V_{\text{row}}^T]^H [h_d, N_V V_{\text{row}}^T]$  so, the received signal power representation as a quadratic form will be  $c^H b c$ . We need to initialize the algorithm  $c_{i+1} = \frac{b c_i}{\|b c_i\|}$  until convergence.

### C. Simulation Results

The simulation results are obtained for different reflecting phase shift per IRS element as per fig(1b). Fig(2) shows

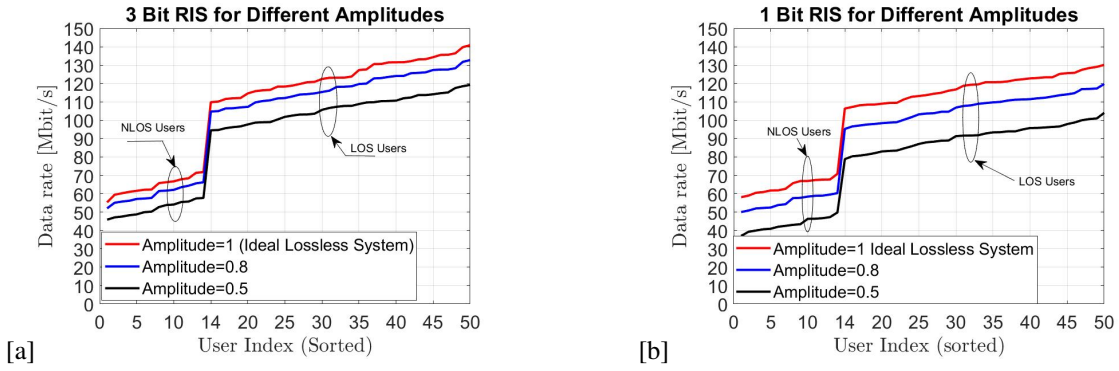


Fig. 3. 3bits and 1bit RIS for Different Amplitude Response

the data rates achieved by the 50 users by setting different reflecting phase spacing per element considering the practical phase shift model in section III. The number of discrete phase shifts at each element are equally spaced and can be given by  $D = (0, \Delta\theta, \dots, \Delta\theta(S-1))$  where  $\Delta\theta = 2\pi/S$  and  $S = 2^q$  and  $q$  the number of bits. It also shows the importance of the RIS technology when compared with the uniform surfaces without considering the IRS configuration. We investigated the performance of three bits RIS to be compared with 1 bit and random phase. We noticed that the data rate increased when the phase levels assigned per each element are increase bearing in mind the equally spaces between the finite number of phases and the reason behind that is The reflective currents are out-of-phase with the element currents when the phase shift is approximately 180 or -180 degrees and so the electric field and current flow in the element are both reduced, resulting in least energy loss and maximum reflection amplitude. The effect of the amplitude response has been taken into account and show its impact on the gain of the data rate unlike many researchers who considered constant amplitude and ignore the related losses. Fig(3a) and (3b) show the impact of amplitude variations on the system data rate performance for three and one bits RIS. Therefore, considering the assumption of lossless amplitude in the literature gives promising results however, energy loss is unavoidable in practical hardware, and the normal behavior of the reflection amplitude is comparable to Fig (1a) hence, a practical phase shift model should be considered taking into account the losses.

#### IV. CONCLUSION

In this paper we demonstrated that RIS can be programmed to result in remarkable performance data rates in comparison with uniform surfaces. Higher discrete phase shifts were compared with one-bit RIS and random phsed to investigate the data rates and we deduced that the data rate boosts up as long as the phase levels assigned per each element increased but the hardware complexity is unavoidable due to the large number of PIN diodes needed per element. The RIS technology is entwined with 6G research so, it is the time to look for refined communication models to leverage the electromagnetic properties that comply with realistic applications.

#### REFERENCES

- [1] C. Liaskos, S. Nie, A. Tsioliaridou, A. Pitsillides, S. Ioannidis, and I. Akyildiz, "A new wireless communication paradigm through software-controlled metasurfaces," *IEEE Communications Magazine*, vol. 56, no. 9, pp. 162–169, 2018.
- [2] Q. Wu and R. Zhang, "Intelligent reflecting surface enhanced wireless network via joint active and passive beamforming," *IEEE Transactions on Wireless Communications*, vol. 18, no. 11, pp. 5394–5409, 2019.
- [3] E. Björnson, H. Wymeersch, B. Matthiesen, P. Popovski, L. Sanguinetti, and E. de Carvalho, "Reconfigurable intelligent surfaces: A signal processing perspective with wireless applications," *arXiv preprint arXiv:2102.00742*, 2021.
- [4] Y. Yang, B. Zheng, S. Zhang, and R. Zhang, "Intelligent reflecting surface meets ofdm: Protocol design and rate maximization," *IEEE Transactions on Communications*, vol. 68, no. 7, pp. 4522–4535, 2020.
- [5] B. Zheng and R. Zhang, "Intelligent reflecting surface-enhanced ofdm: Channel estimation and reflection optimization," *IEEE Wireless Communications Letters*, vol. 9, no. 4, pp. 518–522, 2019.
- [6] E. Björnson, "Optimizing a binary intelligent reflecting surface for ofdm communications under mutual coupling," *arXiv preprint arXiv:2106.04280*, 2021.
- [7] E. Björnson and L. Marcenaro, "Configuring an intelligent reflecting surface for wireless communications: Highlights from the 2021 ieee signal processing cup student competition [sp competitions]," *IEEE Signal Processing Magazine*, vol. 39, no. 1, pp. 126–131, 2021.
- [8] 3GPP. (2020, Jul.) Spatial channel model for multiple input multiple output (mimo) simulations (release 16). [Online]. Available: <https://portal.3gpp.org/desktopmodules/Specifications/SpecificationDetails.aspx?specificationId=1382>
- [9] S. Abeywickrama, R. Zhang, Q. Wu, and C. Yuen, "Intelligent reflecting surface: Practical phase shift model and beamforming optimization," *IEEE Transactions on Communications*, vol. 68, no. 9, pp. 5849–5863, 2020.